

# PROCEEDINGS OF SPIE

[SPIDigitalLibrary.org/conference-proceedings-of-spie](https://spiedigitallibrary.org/conference-proceedings-of-spie)

## Optical characteristics of side-firing fibers for laser prostatectomy

van Vliet, Remco, Molenaar, David, van Swol, Christiaan, Boon, Tom, Verdaasdonck, Rudolf

Remco J. van Vliet, David G. Molenaar, Christiaan F. P. van Swol, Tom A. Boon, Rudolf M. Verdaasdonck, "Optical characteristics of side-firing fibers for laser prostatectomy," Proc. SPIE 2328, Biomedical Optoelectronic Devices and Systems II, (22 December 1994); doi: 10.1117/12.197517

**SPIE.**

Event: International Symposium on Biomedical Optics Europe '94, 1994, Lille, France

# Optical characteristics of side firing fibers for laser prostatectomy

Remco J van Vliet, David G Molenaar, Christiaan FP van Swol,  
Tom A Boon and Rudolf M Verdaasdonk

LASER CENTER



Medical Laser Center and Dept. of Urology,  
University Hospital Utrecht, The Netherlands.

## ABSTRACT

Various side firing fibers have been developed in the past two years for Nd:YAG laser treatment of Benign Prostatic Hyperplasia (BPH). The method to deflect the beam laterally determines the power density at the urethral wall and consequent tissue effects. In this study the optical characteristics of eight different side firing fibers were evaluated by measuring transmission and beam profiles.

A scanning device was developed which consisted of a sensor that was translated in two directions in front of the side firing fiber, while submerged in water. The transmission of the devices was measured by placing them in a transparent water filled tank in front of a power meter.

The scans provided a three dimensional power density distribution of the fibers. The exit angle varied from 41 to 100 degrees, with respect to the fiber axis. The divergence of the beams was different in two directions, resulting in an elliptical spot at the urethral wall. The spot size ranged from 6.6 to 17.5 mm<sup>2</sup> for a clinically relevant situation at 5 mm from the tip. The transmission of a new side firing fiber ranged from 43 to 83 per cent compared to a bare fiber.

Due to the unique optical characteristics of each device, there is a large variation in the power density at the tissue and thus a specific dosimetry protocol for each fiber is required.

## 1. INTRODUCTION

Since the Nd:YAG laser was introduced for the treatment of Benign Prostatic Hyperplasia (BPH) many new devices have become commercially available. Many of them are side firing fibers, that are developed to deflect the laser light at the urethral wall. The treatment dosimetry however in relation to the physical properties of the devices, has not been optimized yet. In this study the optical characteristics of eight side firing fibers have been evaluated in view of optimization of the treatment dosimetry.

## 2. MATERIALS AND METHODS

### 2.1 The various devices and methods of light deflection

The devices that are evaluated are ADD (Laserscope), Laseguide (Laserperipherals), ProLase II (Cytocare), RotaLase (Xintec), Sidefiber (Ceram Optec), SideFire (Myriadlase), Ultraline (Heraeus Lasersonics) and UroLase (Bard). The devices can be classified to their design to deflect light out of the fiber.

### 2.1.1 Deflection by a metal mirror

Light is coupled out of a bare ended fiber onto a gold coated reflector that is positioned in front of it. The UroLase, the RotaLase and the SideFire are based on this principle. At the reflection surface some light will be lost due to absorption. This may lead to heat formation causing an increase of temperature of the fiber tip and a decrease of transmission of the device. The SideFire and the RotaLase incorporate a hole in the metal frame near the mirror of which the manufacturers claim it cools the tip by an induced water flow through the hole along the reflecting surface (Figure 2-1).

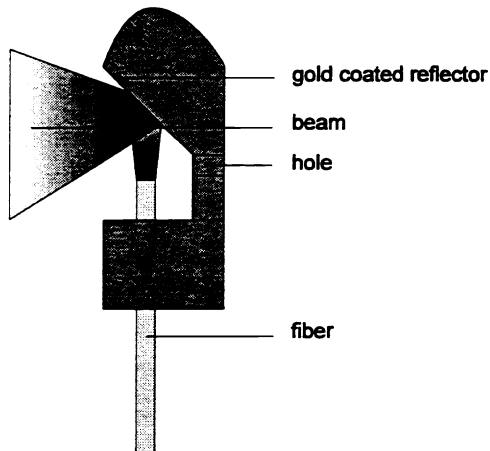


Figure 2-1. Metal reflector tip

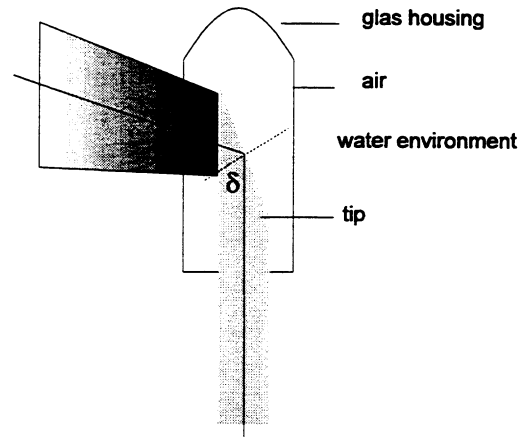


Figure 2-2. Reflection in an angled fiber tip

### 2.1.2 Reflection by total internal reflection

Devices with angled fiber tips make use of total internal reflection caused by a difference in refractive index between the angled tip and the surrounding medium (Figure 2-2).

The end of the fiber is polished at such an angle that rays in the fiber reflect at the angled surface, as their angle of incidence exceeds the critical angle ( $\delta$  in figure 2-1). This critical angle depends on the refractive index of the fiber and the surrounding medium. If the surrounding medium is water the difference of refractive index is too small to obtain a well-defined deflected beam. However, if an air filled capillary is introduced over the angled fiber tip, the rays are deflected if the angle of the tip exceeds the critical angle. The Ultraline, Sidefiber, Laseguide and the ADD are based on this principle. Instead of the silica fiber core a rod of highly refractive material (e.g. sapphire) can be placed in front of a bare fiber ending in an angled tip. Due to the difference of the refractive index with water the air filled capillary is not necessary to deflect the beam in water. The ProLase II is based on this principle. Due to the cylindrical geometry of the fibers that use total internal reflection the deflected beam will have a different divergence in two directions..

## 2.2 Experimental set-up for the optical evaluation.

To determine the optical characteristics of the fiber tips the transmission and the beam profile were measured. A scanning device was developed to measure the beam profile and determine the divergence and the exit angle of the beam.

### 2.2.1 Transmission measurement.

The set-up consisted of a power meter positioned next to a transparent water filled tank. The fiber is placed in such a position that the beam is emitted perpendicular to the surface of the power meter. The advantages of this method are that only the primary beam used for clinical treatment is measured and that high powers used for clinical treatment are possible. This give a good representation of the amount of energy that reaches the tissue.

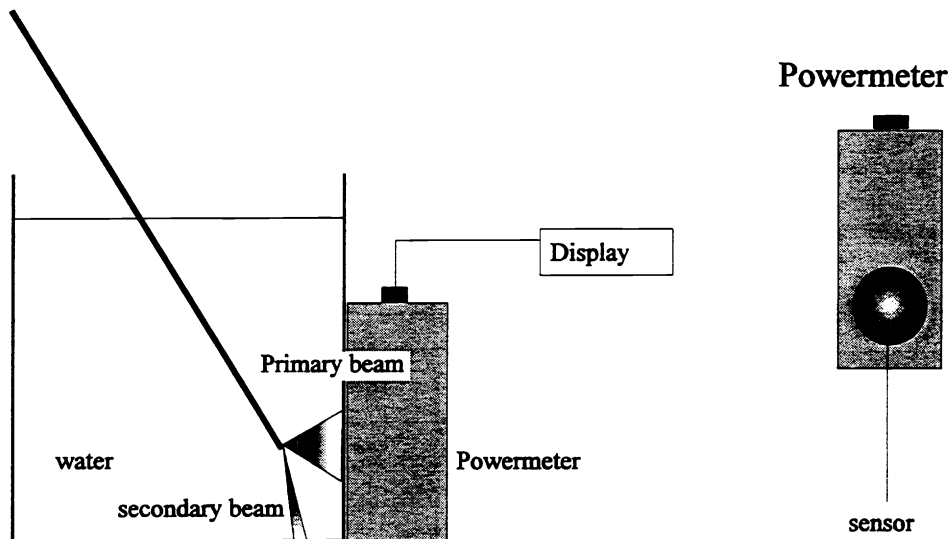


**Figure 2-3. Set up for primary beam transmission**

The measured values are corrected for the reflection caused by the water-glass and glass-air interfaces. A normal incidence is assumed because the distance of the fiber to the cylindrical wall of the tank is small in comparison with the diameter of the cylinder. The correction is calculated using Fresnel's law of reflection<sup>1</sup>.

### 2.2.2 Measurement of the exit angle and divergence

The exit angle and divergence are measured with a scanning device as shown in figure 2-4

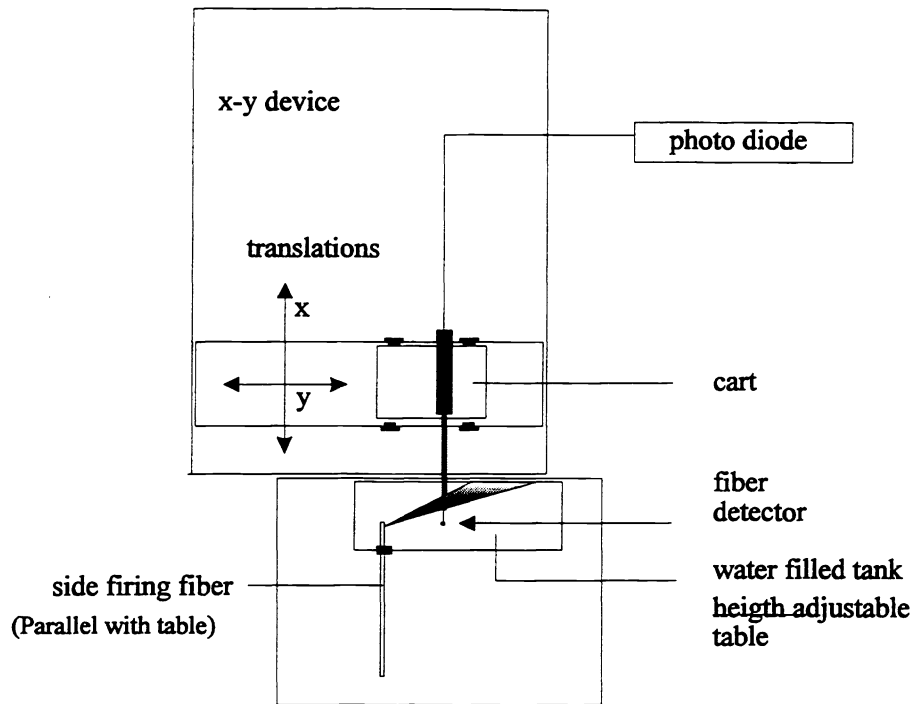


**Figure 2-4. Top view of the scanning device**

The side firing fiber was positioned with its principal axis parallel with or perpendicular to the height adjustable table. The following description is for the parallel positioning (as in Figure 2-4). The fiber tip is submerged in water. The detector is positioned at the same height as the fiber tip using the height adjustable table.

The detector is translated with an x-y device. The x-translator of the x-y device is responsible for the parallel translation. The y-translator moves a small 'cart', which holds the detector. The x and y translations are controlled by analogue signals from a function generator. The signals from the generator and the reading of the detector were the input of a PC based data-acquisition system. The detector was a 60  $\mu\text{m}$  fiber provided with a 80  $\mu\text{m}$  ball shaped tip made of highly scattering material to allow a large acceptance angle.

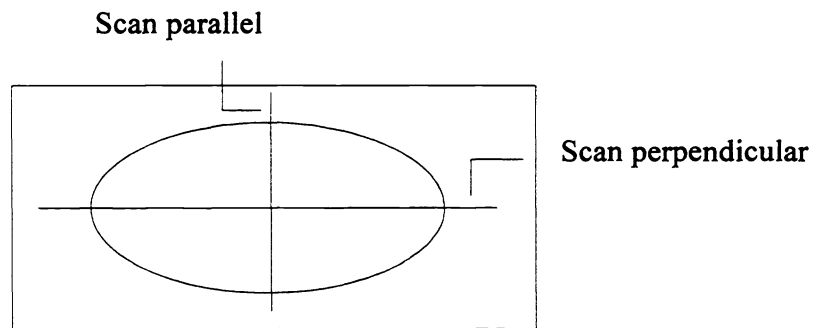


**Figure 2-5. Spot in scan plane**

With the beam profile scanned in two directions it was possible to calculate the divergence of the beam in both directions, parallel and perpendicular to the principal axis. The spot size could then be calculated, assuming the spot to be elliptical<sup>2</sup>.

The exit angle is described as the angle between the axis of maximum intensity in the beam and the principal axis. A beam with an angle higher than 90° is deflected backwards. The divergence is determined at 5 mm from the fiber tip by measuring the beam diameter at the 1/e<sup>2</sup> levels<sup>1</sup> in the beam over a short distance either side of the 5 mm point (Figure 2-6). The determined divergence is the near field divergence.

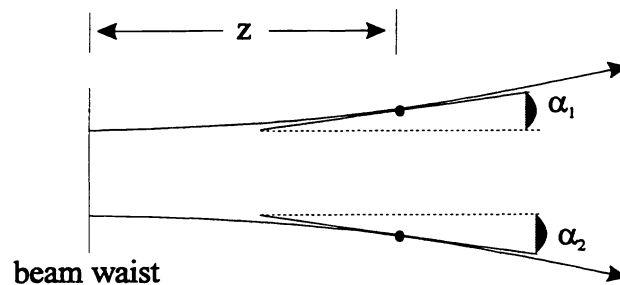


**Figure 2-6. Near field divergence ( $\alpha_1 + \alpha_2$ ) measured at distance  $z$  ( $z=5$  mm)**

### 3. RESULTS

The optical characteristics are determined from the four plots. The contour map and the 3-D plots give an impression of the beam. The fourth plot shows the maxima and the two 1/e<sup>2</sup> contours of the beam. The results are presented in table 2.

The plots of the parallel scan of the UroLase (Bard) are presented as an example. The z-direction in the plot is the direction of the principal axis of the fiber (as in Figure 3-1).

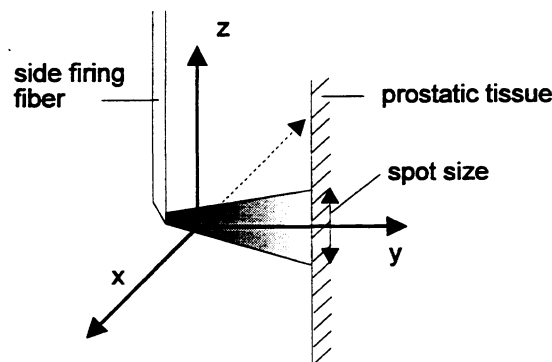


**Figure 3-1. Orientation of the fiber in the plots**

### 3.1 Transmission measurement

The transmission is measured with power input of 40 W compared to the output of a bare fiber. The results of the transmission measurements are presented in the table below.

**Table 1: Transmission results**

<i>fiber</i>	<i>Transmission <math>\pm 1.5</math> [%]</i>	<i>deflection method</i>
Ultraline	83	internal reflection
Laseguide	81	internal reflection
ADD	77	internal reflection
RotaLase	75	Metal reflector
Sidefiber	71	internal reflection
ProLase II	68	internal reflection
UroLase	49	Metal reflector
SideFire	43	Metal reflector

### 3.2 Results of the scan

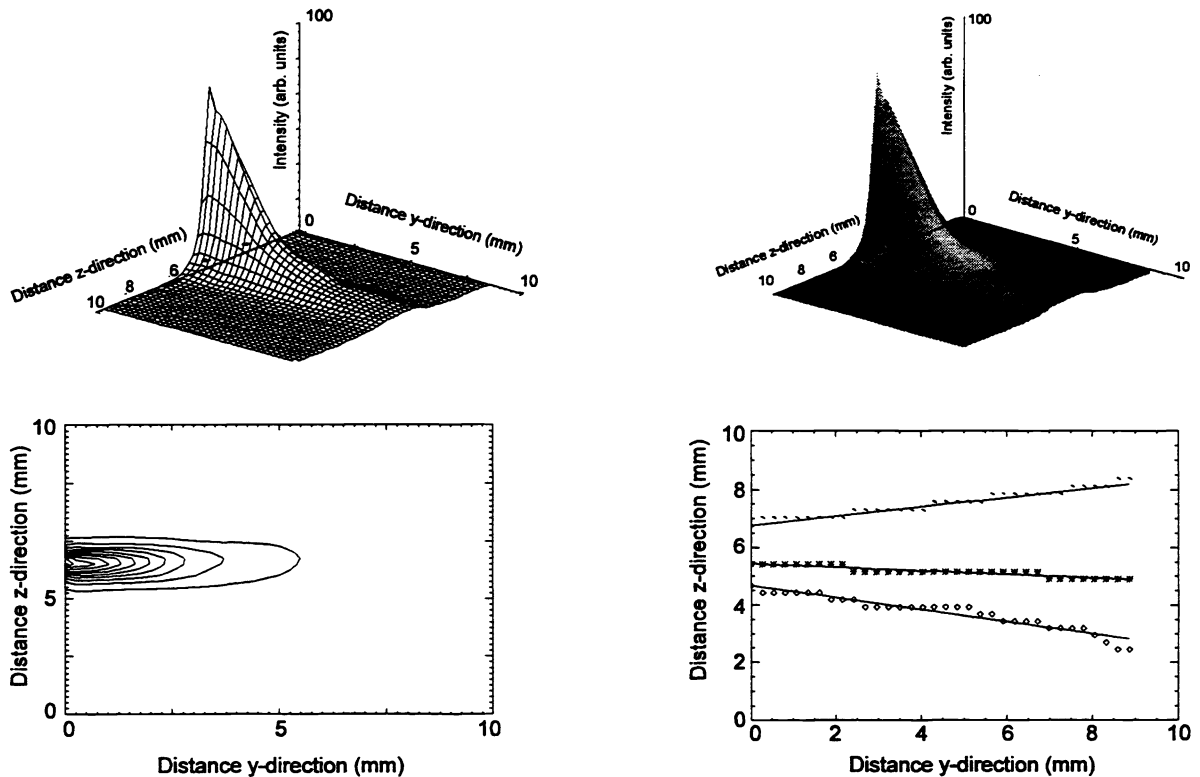


**Figure 3-2. Various plots of the same parallel scan of the UroLase, wire frame, surface map, contour map and plot with  $1/e^2$  divergence lines.**

From the plots the exit angle, divergence and the spot size were determined at 5 mm of the fiber tip.

**Table 2: optical characteristics of the different fibers**

<i>fiber</i>	<i>divergence</i>			<i>spot size</i> [mm <sup>2</sup> ] ± 14%	<i>power density</i> [rel. units]
	<i>exit angle</i> ± 1.5 [°]	<i>perpendicular</i> [°] ± 10%	<i>parallel</i> [°] ± 10%		
ADD	80	23	12	8.3	69
Bare fiber	0	11	11	5.7	100
ProLase II	41	20	15	13.3	43
Laseguide	76	16	9	7.6	75
RotaLase	90	16	13	8.9	64
Sidefiber	77	22	13	9.6	59
SideFire	100	15	13	10.5	54
Ultraline	82	15	10	6.6	86
UroLase	87	37	24	17.5	33

#### 4. DISCUSSION

The power density distribution was measured using a scanning device. From the obtained distribution various optical characteristics could be determined. The spot size was assumed to be elliptical and for most devices this assumption was reasonable. However, due to the conical shape of the metal reflector of the UroLase the shape of the spot looks more like a banana. Therefore the real spot size is smaller than calculated.

The geometry of the prostate was assumed cylindrical and the fiber was supposed to be held parallel to the tissue surface. In reality the prostate is more humpbacked, so the fiber is not always parallel to the surface. Further it is sometimes troublesome for the physician to keep the fiber parallel to and at a fixed distance from the tissue. These two effects influence the spot size and thus the power density: if the fiber is positioned not parallel to the tissue but under a certain angle, the spot size will become larger and the power density will decrease. If the distance between fiber and prostatic tissue decreases the power density grows rapidly. The tissue effects will differ accordingly.

If the transmission results are compared with temperature measurements<sup>3</sup> the results are in agreement with each other. The fibers with the lowest transmission reaches the highest temperature (100°C by 40 W power input). Basically, the differences between the devices are due to the method of beam deflection and the use of metal parts in the construction of the fiber tip. The devices which use total internal reflection have a higher transmission than the metal mirror devices. Metal parts, used to shield possible secondary beams, give rise to light absorption and consequently become heated.

All the devices that were measured were new. The clinical use of the devices causes them to deteriorate, consequently the beam profile may change. During use with high input power little vapor bubbles develop at the tip. The beam will be scattered, so light is spread over a large area and the temperature of the tip will rise as these bubbles prevent it from being cooled by the surrounding water. The latter may even cause permanent damage to the device. Also new fibers can induce vapor bubbles by high input power and the transmission loss can be dramatic (up to 50 %). Therefore transmission measurement should be done with high input power.



## 5. CONCLUSION

The optical characteristics of the various laser devices introduced for BPH treatment differ strongly. Consequently, the power density of the laser beam on the prostatic tissue varies depending on the devices and their distance to the tissue. This has substantial consequences on the desired tissue effects and the method of application.

## 6. ACKNOWLEDGMENTS

The authors wish to thank Mr. H.J. Mansvelt Beck for the construction of the scanning device.

## 7. REFERENCES

1. E. Hecht, Hecht Optics, pp. 99-104, Addison Wesley Publishing Company, Amsterdam, 1987.
2. C.F.P. van Swol, R.M. Verdaasdonk, J. Mooibroek, T.A. Boon, "Physical evaluation of laser protatectomy devices", Lasers in Urology, G.M. Watson, R.W. Steiner, D.E. Johnson (eds.), Vol. 2129, pp. 25-33, SPIE, Bellingham, 1994.
3. D.G. Molenaar, R.J. Van Vliet, R.M. Verdaasdonk, T.A. Boon, C.F.P. van Swol, "Evaluation of laser prostatectomy devices by thermal imaging", Interstitial thermotherapy, S. Bown, F. Frank, T.J. Vogl (eds.), Vol. 2327, SPIE, Bellingham, 1994 (in press).